



PCCP

One-electron oxidation of ds(5'-GGG-3') and ds(5'-G(8OG)G-3') and the nature of hole distribution: A density functional theory (DFT) study

Journal:	<i>Physical Chemistry Chemical Physics</i>
Manuscript ID	CP-ART-11-2019-006244.R2
Article Type:	Paper
Date Submitted by the Author:	30-Jan-2020
Complete List of Authors:	Kumar, Anil; Oakland University, Chemistry Adhikary, Amitava; Oakland University, Chemistry Sevilla, M.; Oakland University, Chemistry Close, David; East Tennessee State University, Physics and Astronomy

SCHOLARONE™
Manuscripts

One-electron oxidation of ds(5'-GGG-3') and ds(5'-G(8OG)G-3') and the nature of hole distribution: A density functional theory (DFT) study†

Anil Kumar^a, Amitava Adhikary^a, Michael D. Sevilla*^a, and David M. Close^b

^aDepartment of Chemistry, Oakland University, Rochester, Michigan 48309, USA.

^bDepartment of Physics, East Tennessee State University, Johnson City, Tennessee 37614, USA.

Abstract

Of particular interest in radiation-induced charge transfer processes in DNA is the extent of hole localization immediately after ionization and subsequent relaxation. To address this, we considered double stranded oligomers containing guanine (G) and 8-oxoguanine (8OG), i.e., ds(5'-GGG-3') and ds(5'-G8OGG-3') in B-DNA conformation. Using DFT, we calculated a variety of properties, viz., vertical and adiabatic ionization potentials, spin density distributions in oxidized stacks, solvent and solute reorganization energies and one-electron oxidation potential (E°) in the aqueous phase. Calculations for the vertical state of the -GGG- cation radical showed that the spin was found mainly (67%) on the middle G. However, upon relaxation to the adiabatic -GGG- cation radical, the spin localized (96%) to the 5'-G, as observed in experiments. Hole localizations on the middle G and 3'-G were higher in energy by 0.5 kcal/mol and 0.4 kcal/mol respectively than that of 5'-G. In -G8OGG- cation radical, the spin localized only on the 8OG in both vertical and adiabatic states. The calculated vertical ionization potentials of -GGG- and -G8OGG- stacks were found to be lower than that of the vertical ionization potential of a single G in DNA. The calculated E° of -GGG- and -G8OGG- stacks are 1.15 and 0.90 V which owing to stacking effects are substantially lower than the corresponding experimental E° values of their monomers (1.49 and 1.18 V). SOMO to HOMO level switching is observed in these oxidized stacks. Consequently, our calculations predict that local double oxidations in DNA will form triplet diradical states which are especially significant for high LET radiations.

† Electronic supplementary information (ESI) available: Supporting information contains the following: (i) Structure of ds(5'-GGG-3') and ds(5'-G8OGG-3'). (ii) Table. (iii) Scheme. (iv) Plots of MOs and (v) optimized geometries.

Introduction

The direct interaction of ionizing radiation with DNA randomly ionizes and forms “holes” (cation radicals) on each of its component (i.e. bases, sugar and phosphate). - The holes travel within DNA by tunneling and by thermally-activated hopping processes and localize on the DNA base having the lowest ionization potential (IP), guanine, forming the guanine radical cation ($G^{\bullet+}$).¹⁻⁹ Electron spin resonance (ESR) and product analyses experiments showed that via nucleophilic addition of a water molecule at the C8 site of $G^{\bullet+}$ followed by deprotonation leads to the formation of highly reducing $G8OH\bullet$ intermediate; subsequent one-electron oxidation of $G8OH\bullet$ followed by deprotonation produces 8-oxoguanine (8OG) which has a lower IP than G and acts as a global sink for hole traps in one electron oxidized DNA.¹⁰⁻¹⁴

Factors such as base-pairing, stacking and solvation surrounding the DNA significantly affect the ionization potentials of bases in DNA. The photoionization of nucleosides and nucleotides in water has been studied in several pulsed laser experiments with 282¹⁵, 266^{16,17}, 254¹⁸ and 193 nm¹⁹ photons which bracketed the threshold ionization limit of DNA components between 4.40 – 6.42 eV, respectively. Microhydration of A and T are shown to reduce the IP of these bases by ca. 0.7 eV than their gas phase values²⁰. Under full aqueous solvation, Lebreton and coworkers²¹ established ionization threshold of ca. 4.8 eV for guanine. Experimentally measured IPs were further supported by theory carried out by Close and coworkers²²⁻²⁴, Jungwirth and coworkers²⁵⁻²⁷ and Capobianco et al.²⁸ including aqueous solvent environment on DNA bases via either consideration of explicit solvation model (polarized continuum model (PCM)) or by placing discrete water molecules around bases. The ionization potentials of hydrogen-bonded GC and AT base pairs in the gas phase and in solution were calculated using HF and DFT methods by Colson et al.²⁹⁻³¹, Li et al.^{32,33}, Hutter and Clark³⁴, Kumar and Sevilla⁹ and by Bravaya et al.³⁵ using the high level EOM-IP-CCSD/6-311+G(d,p) method. Their calculations showed that hydrogen-bonded DNA bases have lower IPs than monomeric bases.^{9,29-35} Theoretical calculations also showed that stacked DNA bases have lower IPs than monomeric bases.³⁵⁻⁴¹ As found by Ab initio EOM-IP-CCSD calculations by Krylov and coworkers^{35,40,41} of the IP_{vert} of stacked UU, AA, TT and AATT tetramers. Very recently, differential pulse voltammetry (DPV) measurements of

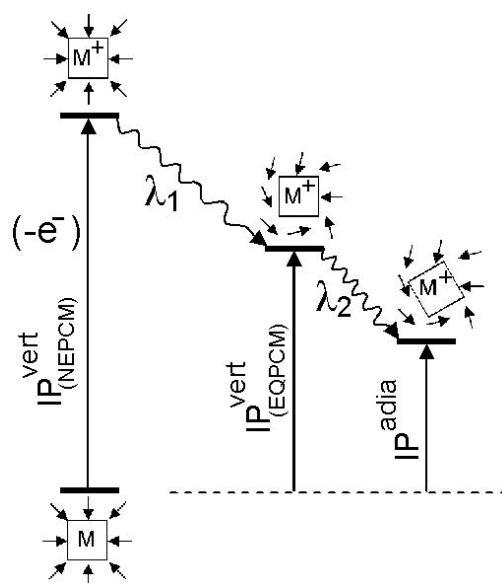
guanine-rich single- and double-stranded oligonucleotides containing up to six consecutive guanines are reported by Capobianco et al.⁴² and they observed progressive lowering of the first voltammetric peak potential as the number of guanines increases. Using photoelectron spectroscopy and MP2/aug-cc-pvdz calculations the vertical IP of DNA in aqueous solution were very recently estimated by Jungwirth and coworkers⁴³ and they concluded that the lowest IP_{vert} (ca. 7 eV) corresponds to the guanine base in DNA.

IPs of DNA and its bases in various configurations have been extensively studied using quantum chemical methods^{13,14,22,35} and an excellent agreement between theory and experiment is achieved. However, in the context of ionization (oxidation event) of DNA, the nature of hole distribution in DNA is of prime importance. There is a marked difference of opinion on whether the hole is localized on a single base^{28,38,39,44-51} or is delocalized over a few bases.^{42,52-56} Using theory and experiment, Saito and coworkers^{39,44} demonstrated that sequences of 5'-GG-3' and 5'-GGG-3' in DNA are the sites having the lowest IPs in DNA and the molecular orbitals, calculated by HF/3-21G* method, are mainly localized on the 5'-G with a small amount resides on 3'-G on a stacked *N*-methylated GG/CC system. Barton and coworkers⁴⁵ showed that the photo-oxidation of rhodium intercalator covalently attached to one end of the DNA produces long-range oxidative damage at the 5'-G of DNA containing 5'-GG-3' doublets. Recently, the one-electron oxidized DNA-oligomers were studied using electron spin resonance (ESR) experiment at 77 K by Adhikary et al.⁴⁶ In this experiment, the site of hole localization was determined by use of oligomers with deuterium substitution at the C8 position of guanine at selected sites in the DNA sequences. ESR experiments⁴⁶ clearly showed that the hole is mostly localized at the 5'-G end in deuterium substituted oligomers containing -GGG- sequences. These experimental observations were further supported by several theoretical studies.^{28,37,38,47-49,51} Blancafort and Voityuk⁴⁷ used CASSCF and CASPT2 level of theories to calculate the Mulliken charges of one-electron oxidized several G stacked nucleobases and they found more than 95% of holes are localized on the 5'-G. Senthilkumar et al.⁴⁸ used DFT to calculate the charges distribution on 5'-XGGGY-3' (X, Y = A, C, T) duplexes and concluded that 5'-G is the most easily oxidized. However, there are a few studies that proposed delocalized nature of the hole distribution in G-stacks.^{42,52-54} Liu and Schuster⁵² proposed that long-range hole transfer

in irradiated anthraquinone-linked duplex DNA oligomers mediates via thermally activated polaron-like hopping in DNA and causing formation of 8OG at -GG- steps revealed ultimately as strand breaks. From the progressive lowering of the oxidation potential as the number of stacked guanines increases up to six, Capobianco et al.⁴² proposed the delocalization of the hole on Gs.

To address the issue of the extent of hole (unpaired spin) localization immediately after ionization (vertical) and after relaxation (adiabatic), we considered double stranded ds(5'-GGG-3') and damaged ds(5'-G8OGG-3') (8OG= 8oxoG) in B-DNA conformations and calculated their vertical and adiabatic ionization potentials and spin density (hole) distributions within these stacks under the influence of an aqueous solution. From spin density plots, we analyzed the nature of hole distributions in -GGG- and damaged -G8OGG- stacks and the effect of solvent relaxation on the hole distributions in these stacks. In addition, we report separate reorganization energies of solvent (λ_1) and solute (λ_2) for stacks of -GGG- and -G8OGG- (scheme 1). Another important aspect known as SOMO-HOMO level inversion, observed experimentally⁵⁵⁻⁵⁷ in several radicals and first shown by Coote and co-workers⁵⁸⁻⁶¹ using ab initio and DFT calculations and later by us^{9,61}, is also found to occur for these systems. SOMO-HOMO level switching in radicals has important implications for the redox chemistry of radicals.⁵⁵⁻⁶¹

It is well known that holes produced in oxidized DNA end up on G, GG and GGG sites with the multiple G sites favored for hole localization.^{28,37,39,44 - 48} Moreover, 8OG owing to its lower redox potential¹¹ than those of G sites, becomes favored for hole localization when present. Therefore, owing to computational limitations, we have chosen ds(5'-GGG-3') and ds(5'-G8OGG-3') systems as models of larger DNA systems^{42,46} which have -GGG and -G8OGG- sequences to investigate hole localization in DNA. We note that the sequence context around the GGG sites can influence the specific site of hole localization.⁴⁸



Scheme 1- Schematic diagram showing the procedure for calculation of the vertical and adiabatic ionization potentials of a molecule (M) (solute) in solution by one-electron oxidation of the parent solute molecule (M) under specific conditions. The different quantities depicted in the scheme are defined as: (a) $IP_{(NEPCM)}^{vert}$ This is the vertical IP in which the geometrical configuration of oxidized (M^+) is identical to the neutral (M) including solvent polarization shown by arrows. (b) $IP_{(EQPCM)}^{vert}$ This is the vertical IP in which the geometrical configuration of M^+ is identical to parent M but the surrounding solvent is relaxed in response to the molecular charge formed on ionization. (c) IP^{adia} This is the adiabatic IP in which M^+ and surrounding solvent are fully relaxed. (d) The difference between $IP_{(NEPCM)}^{vert}$ and $IP_{(EQPCM)}^{vert}$ gives an estimate of the solvent reorganization energy (λ_1). and (e) The difference between $IP_{(EQPCM)}^{vert}$ and IP^{adia} gives solute reorganization energy (λ_2). The full reorganization energy, $\lambda_{total} = \lambda_1 + \lambda_2 = IP_{(NEPCM)}^{vert} - IP^{adia}$.

Methods of Calculation

The initial structures of ds(5'-GGG-3') and ds(5'-G8OGG-3') were generated using the SPARTAN program.⁶² The anionic phosphate groups in these stacks were protonated to neutralize the system and 5'- and 3'-ends were terminated by OH groups. The structures thus generated were fully optimized in their neutral state by ω B97XD density functional using the 6-31G** basis set. The fully optimized neutral state geometries of ds(5'-GGG-3') and ds(5'-G8OGG-3') were used for the calculation of the vertical and adiabatic ionization potentials of these stacks using similar calculation levels. All the calculations were carried out in the aqueous phase via the integral equation formalism of the polarized continuum model (IEF-PCM) by Tomasi et al.⁶³ For IEF-PCM

calculations the solvent treated as a continuum and the cavity was generated using the default options set into the program. The complete methodology in the present work is abbreviated as ω B97XD-PCM/6-31G**. The ω B97XD is a range-separated hybrid density functional with damped atom–atom dispersion corrections developed by Chai and Head-Gordon.^{64,65} This functional has been found reliable for the calculation of various properties of molecules in their ground and excited states in our recent works^{9,13,66,67} and by others.³⁵ Using the ω B97XD-PCM/6-31G** optimized geometries the calculation level were further increased by calculating the ionization potentials using the 6-31++G** basis set. The complete optimization of structures with the 6-31++G** basis set is beyond our computational resources. All the calculations were carried out using the Gaussian 16 suite of programs.⁶⁸ Figures S1 – S13 and Table S1 – S3 are presented in the supporting information. We also carried our ab initio molecular dynamics (MD) simulation starting with the vertical radical cation of -GGG- stack using the ω B97XD-PCM/6-31G** method. The details of the MD simulations and results are presented in the supporting information.

To check the reliability of ω B97XD-PCM/6-31++G**// ω B97XD-PCM/6-31++G** methodology, we calculated the ionization potentials and relaxation energies λ_1 and λ_2 of the guanine and 8oxoguanine monomers and compared them to those calculated using the MP2/aug-cc-pVDZ method by Jungwirth and coworkers,^{26,69,74} and ourselves. We found that the calculated IPs and relaxation energies with both methods are in excellent agreement see Tables S2 and S3 in the supporting information.

The procedure for calculation of the vertical and adiabatic ionization potentials of a molecule (M) (solute) in the presence of a solvent (shown by arrows) is shown in scheme 1. From scheme 1, it is evident that in the calculation of the vertical IP, we considered the effect of solvent in two ways: (i) Nonequilibrium solvent - In this case only the fast electronic response of the solvent was considered while the nuclear response was constrained to the optimized solute (M) with PCM before ionization.^{27,69} This protocol is known as nonequilibrated PCM (NEPCM) and implemented in the Gaussian program.⁶⁸ The vertical IP in this state is designated as $IP_{(NEPCM)}^{vert}$. and (ii) Equilibrated solvent- In this case, solvent was allowed to relax but solute was constrained to the optimized solute

(M) before ionization. This protocol is termed as equilibrated PCM (EQPCM) in this study. The vertical IP in this state is designated as $IP^{\text{vert}}_{(\text{EQPCM})}$. The adiabatic IP (IP^{adia}) is calculated as the energy difference between the optimized solute (M) with a relaxed PCM (EQPCM) after and before ionization. The reorganization energy of the solvent (λ_1) and of the solute (λ_2) are estimated as: $\lambda_1 = IP^{\text{vert}}_{(\text{NEPCM})} - IP^{\text{vert}}_{(\text{EQPCM})}$; $\lambda_2 = IP^{\text{vert}}_{(\text{EQPCM})} - IP^{\text{adia}}$. The sum ($\lambda_1 + \lambda_2$) gives the total reorganization energy (λ_{total}) due to relaxed solute and solvent, respectively.

Results and Discussion

Aqueous phase ionization and oxidation potentials- The $\omega\text{B97XD-PCM/6-31G}^{**}$ calculated vertical and adiabatic ionization potentials of ds(5'-GGG-3') oligos in the B-DNA conformation is given in Table S1 in the supporting information.

The calculated $IP^{\text{vert}}_{(\text{NEPCM})}$, $IP^{\text{vert}}_{(\text{EQPCM})}$ and IP^{adia} of ds(5'-GGG-3') at $\omega\text{B97XD-PCM/6-31++G}^{**}/\omega\text{B97XD-PCM/6-31G}^{**}$ level of theory are 6.64, 5.96 and 5.59 eV, respectively, see Table 1. Our calculated $IP^{\text{vert}}_{(\text{NEPCM})}$ (6.64 eV) of ds(5'-GGG-3') by $\omega\text{B97XD-PCM/6-31++G}^{**}$ is about 0.4 eV lower than the $IP^{\text{vert}}_{(\text{NEPCM})}$ of a single guanine base in DNA dodecamer calculated using *ab initio* MP2/aug-cc-pvdz level of theory considering the ONIOM approach in Gaussian suite of programs⁶⁸ and estimated experimentally using valence photoelectron spectra of sheared herring sperm DNA at pH 7.7 by Jungwirth and coworkers.⁴³ This difference (0.4 eV) is evident as our calculated $IP^{\text{vert}}_{(\text{NEPCM})}$ is of stacked -GGG- while the later is calculated for a single guanine in DNA. The calculated IP^{adia} (5.59 eV), see Table 1) of -GGG- is ca. 1.1 eV less than the $IP^{\text{vert}}_{(\text{NEPCM})}$. This lowering of IP results from the solvent and solute relaxation. The lower IP of stacked -GGG- in comparison to single guanine are also reported in earlier studies.³⁷⁻³⁹ Very recently, DPV (Differential Pulsed voltametry) measurements showed lowering of 0.1 V oxidation potential in per GG step in single- and double-stranded DNA containing up to six consecutive stacked guanines.⁴² This gives us an indication that -GGG- sequence has lowering in oxidation potential between 0.15 – 0.2 V. The one-electron oxidation potential (E°) of G is 1.49 V with (E_7) 1.29 V^{1,69,70} and thus the estimated E° of -GGG- should be ca. 1.3 V. The one-electron reduction potential (E°) is calculated as $E^{\circ} = (-\Delta G) - \text{SHE}$ (standard hydrogen electrode). The negative of free

energy (ΔG) is simply the adiabatic ionization potential in aqueous phase (IP^{adia}) referenced to the SHE rather than vacuum.⁶⁹ Thus, our calculated E° of -GGG- is $5.59 \text{ V} - 4.44 \text{ V(SHE)}^{71-73} = 1.15 \text{ V}$, which is only in reasonable agreement with the experimental estimate of 1.3 V of -GGG- stack, see Table 1. The calculations of E° using both the methods are reported in the supporting information (see Table S1).

The ω B97XD-PCM/6-31++G**// ω B97XD-PCM/6-31G** calculated $IP^{vert}_{(NEPCM)}$, $IP^{vert}_{(EQPCM)}$ and IP^{adia} of ds(5'-G8OGG-3') are 6.43, 5.74 and 5.34 eV, respectively. It is evident from Tables 1 that the IPs of -G8OGG- stack are ca. 0.2 eV lower than the corresponding IPs of -GGG- stack. Palivec et al.⁷⁴ calculated the $IP^{vert}_{(NEPCM)}$ (6.94 eV) of single 8OG using PMP2/aug-cc-pVDZ level of theory which is ca. 0.5 eV higher than our calculated $IP^{vert}_{(NEPCM)}$ of ds(5'-G8OGG-3'), see Table 1. This difference is expected as our calculation of IP is for ds(5'-G8OGG-3') which involves stacking and hydrogen-bonding interactions while the calculations of Palivec et al.⁷⁴ are for single 8OG. The lower IP of -G8OGG- than -GGG- (see, Tables 1 and S1) is in accord with experimental observations as 8OG is found to be a better hole trap (oxidation site) than G in DNA on one-electron oxidation.¹⁰⁻¹⁴ The calculated E° of -G8OGG- stack is $5.34 - 4.44 = 0.90 \text{ eV}$, see Table 1. Using kinetic rate measurement, Steenken et al.¹¹ measured the E° of 8-oxoG in aqueous solution as 1.18 V.

Table 1- ω B97XD-PCM/6-31++G**// ω B97XD-PCM/6-31G** calculated vertical and adiabatic ionization potentials and relaxation energies (λ_1 , λ_2 , and λ_{total}) of ds(5'-GGG-3') and ds(5'-G8OGG-3') oligos in eV. The estimated oxidation potential E° is given in volts.

System	ω B97XD-PCM/6-31++G**// ω B97XD-PCM/6-31G** ^a						$E^{\circ,b}$	Exp
	$IP^{vert}_{(NEPCM)}$	$IP^{vert}_{(EQPCM)}$	IP^{adia}	λ_1	λ_2	λ_{total}		
ds(5'-GGG-3')	6.64	5.96	5.59	0.68	0.37	1.05	1.15	“1.3” ^c
ds(5'-G8OGG-3')	6.43	5.74	5.34	0.69	0.4	1.09	0.90	1.18 ^d

^aAll values in eV except E° in volt.

^b $E^{\circ} = IP^{vert}_{(NEPCM)} - \lambda_{total} - \text{SHE}$; $IP^{adia} = IP^{vert}_{(NEPCM)} - \lambda_{total}$; SHE = 4.44 volt.

^cEstimated from DPV measurements showed lowering of 0.1 V oxidation potential per GG step in both single- and double-stranded DNA, i.e. 1.5 V(G)- 0.2 V (GGG).⁴²

^d8-oxoG (monomer).¹¹

Relaxation energies and spin density distributions- The ω B97XD-PCM/6-31++G**// ω B97XD-PCM/6-31G** calculated solvent relaxation energy (λ_1) of ds(5'-GGG-3') and ds(5'-G8OGG-3') cation radicals are the same and these are 0.68 and 0.68 eV, respectively, see Table 1. In this context, the solvent relaxation energies (λ_1) for A, T, G, C and uracil nucleosides and nucleotides in PCM were estimated as 1.1 eV for all the bases by Schroeder et al.⁶⁹ using the MP2/aug-cc-pVDZ level of theory. Our and Schroeder et al.⁶⁹ studies clearly indicate that the solvent response depends on the overall shape of the electronic distribution of solute on ionization and this is clearly evident that spin density distributions of ds(5'-GGG-3') and ds(5'-G8OGG-3') cation radicals calculated in NEPCM and EQPCM all have a π -type MO with delocalization on one base with lesser contributions from other bases, see Figures 1 - 3 and S4 in the supporting information. The solute relaxation energy (λ_2) calculated by ω B97XD-PCM/6-31++G**// ω B97XD-PCM/6-31G** level of theory for ds(5'-GGG-3') and ds(5'-G8OGG-3') are 0.37 and 0.4 eV, respectively, see Table 1. Using MP2/aug-cc-pVDZ level of theory⁶⁹, λ_2 of guanosine and 5'-guanosine monophosphate (5'-GMP) cation radicals in PCM were calculated as 0.44 and 0.45 eV, respectively, and these values are in good agreement with our calculated λ_2 (0.37 eV) of ds(5'-GGG-3'). The experimental λ_2 in the gas phase for guanine cation radical is 0.47 eV and this is well-predicted by several theoretical calculations.⁷⁵

The spin density distributions of one-electron oxidized ds(5'-GGG-3'), calculated in NEPCM and EQPCM in the vertical states and finally the optimized cation radical in the adiabatic state using ω B97XD-PCM/6-31G** are shown in Figure 1. From Figure 1(a), we see that for NEPCM the spin is delocalized over two bases with the middle G with 62% and 5'-G with 35% of the spin density. When the solvent is allowed to relax in the vertical state (EQPCM) the spin density distribution redistributes significantly in comparison to NEPCM (see Figure 1(a)) and 5'-G has 85% and middle G has 15% of the total spin density, see Figure 1(b). Changing from NEPCM to EQPCM in the vertical state, the PCM-calculated solvent polarization shifts from the polarization inherent in the neutral structure to that for the cation radical. This has a significant effect on the spin distribution within -GGG- stack. This occurs within a few picoseconds as the solvent

equilibrates to the charge. Finally, for the full optimization of the radical cation (adiabatic state with PCM) 95% of the total spin is localized on the 5'-G, see Figure 1(c).

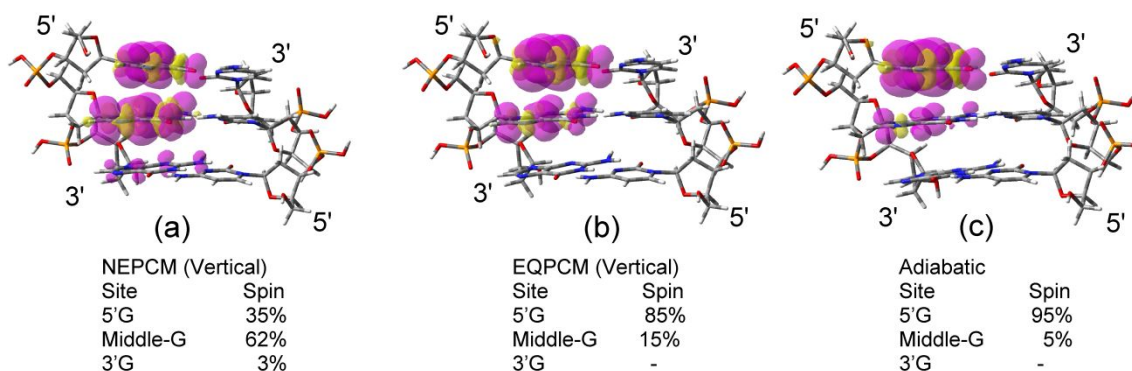


Figure 1. Spin density plots of one-electron oxidized ds(5'-GGG-3') calculated using the $\omega b97xd\text{-PCM}/6\text{-}31G^{**}$ level of theory. (a) in NEPCM, (b) in EQPCM and (c) finally the fully optimized cation radical (adiabatic).

The $\omega B97XD\text{-PCM}/6\text{-}31++G^{**} // \omega B97XD\text{-PCM}/6\text{-}31G^{**}$ calculated spin density distributions in vertical and in adiabatic states of one-electron oxidized ds(5'-GGG-3') are presented in Figure 2. In NEPCM the spin is delocalized on 5'-G (28%) and on the middle G (67%), see Figure 2(a). In EQPCM, the spins on 5'-G and the middle G are 37% and 60%, respectively, see Figure 2(b). The $\omega B97XD\text{-PCM}/6\text{-}31++G^{**} // \omega B97XD\text{-PCM}/6\text{-}31++G^{**}$ calculation shows that on solvent relaxation in the vertical state (EQPCM) spin density transfers from the middle G to 5'-G mildly in comparison to

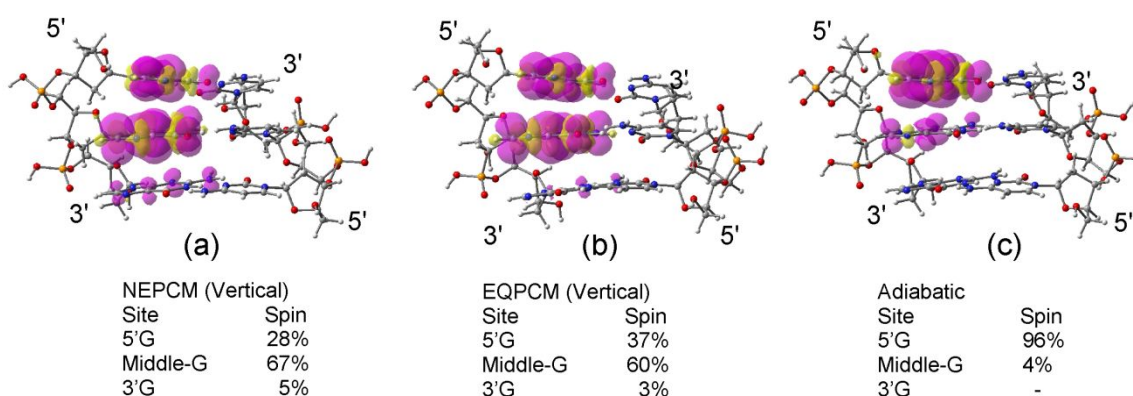


Figure 2. Spin density plots of one-electron oxidized ds(5'-GGG-3') calculated using the $\omega b97xd\text{-PCM}/6\text{-}31++G^{**} // \omega b97xd\text{-PCM}/6\text{-}31G^{**}$ method. (a) in NEPCM, (b) in EQPCM and (c) finally the fully optimized cation radical (adiabatic).

ω B97XD-PCM/6-31G** method, see Figures 1(b) and 2(b), but both the methods propose the transfer of spin towards 5'-G. In the adiabatic state, 96% spin is localized on 5'-G only. The complete localization (95%) of total spin density on 5'-G in (5'-GGG-3') in the adiabatic state (Figure 1(c) and 2(c)) is in agreement with several studies including both theory and experimental results.^{28,38,39,44–51} Our calculations predict a localized hole on 5'-G in an adiabatic radical cation –GGG- stack. Voityuk⁷⁶ also concluded that cation radical states in DNA sequences are localized to single G because of solvation and reorganization effects but the site was sequence dependent. For example, in the sequence AG₁G₂G₃ the hole initially was on both G₁G₂ and on full solvation the hole localized only on G₂. Counter ions also affect the site of hole localization. For example, Barnett et al.⁷⁷ using QM/MM calculations reported that hydrated counter ions (i.e. Na⁺) strongly affect the energetics of an electron hole states in DNA.

The spin density distributions in one-electron oxidized ds(5'-G8OGG-3') in NEPCM and in EQPCM in the vertical states and finally in the adiabatic state, calculated by both the methods, are shown in Figures 3 and S4 in the supporting information. From Figures 3 and S4, we see that the spin is almost completely localized on 8OG in every case, i.e., NEPCM (85%), EQPCM (90%) and for the adiabatic cation radical (90%) of the total spin, see Figures 3 and S4 in the supporting information.

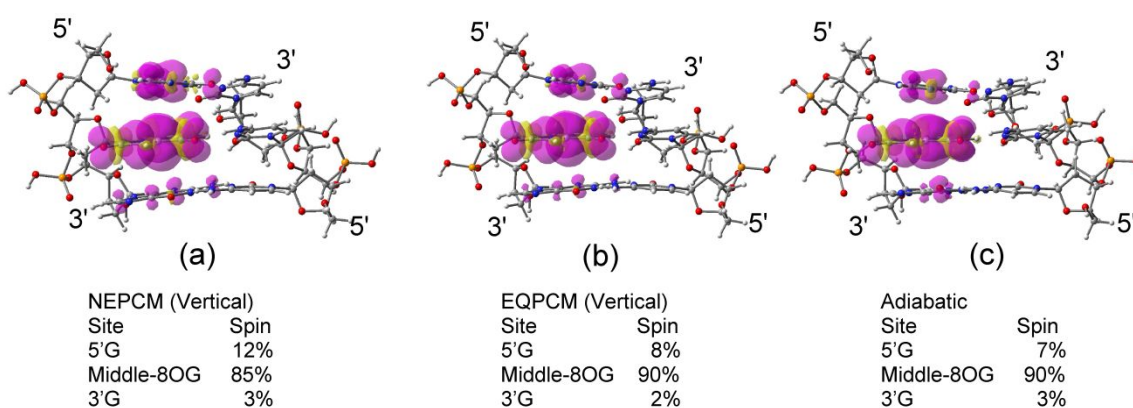


Figure 3. Spin density plots of one-electron oxidized ds(5'-G8OGG-3') calculated using the ω b97xd-PCM/6-31++G**// ω b97xd-PCM/6-31G** method. (a) in NEPCM, (b) in EQPCM and (c) fully optimized cation radical (adiabatic).

It is well known that DFT (such as B3LYP) suffers from self-interaction error (SIE) which leads to spin delocalization⁵¹. However, in range separated hybrid DFT methods (ω b97xd), the problem of SIE is largely mitigated. Since the Hartree-Fock (HF) methodology is free from SIE problem, we have checked whether our ω b97xd calculated spin densities shown in Figures 1 – 3 are affected by SIE. We further calculated the spin densities using the HF-PCM/6-31++G**// ω b97xd-PCM/6-31G** level of theory. The calculated spin densities of ds(5'-GGG-3') and ds(5'-G8OGG-3') cation radical stacks are presented in Figures S7 and S8 in the supporting information. The HF calculated spin density of ds(5'-GGG-3') cation radical in NEPCM and in EQPCM shows that spin is mainly localized on the middle G while in adiabatic cation radical the spin is localized on the 5'-G, see Figure S7 in the supporting information. For ds(5'-G8OGG-3') stack cation radical, spin is only localized on the 8OG. Thus, both HF and ω b97xd methods predict similar spin density distributions.

Why does hole localize on 5'-G ?

The question arises why is 5'-G localization chosen over other G sites in the –GGG- stack. Previous works^{37,47,48,51,76} on G stacks show that localization to a single G occurs on relaxation of solvent and structure. So, it would seem likely that the 5'-G site is the energetically favored position. To test this, we performed calculations that localized the holes first to the central G and subsequently to the 3'-G. The procedures used for these two calculations are: (i) To localize the hole on the central G we replaced the central G with the bond lengths found for the 5'-G cation radical and the 5'- and 3'-Gs were kept in the neutral geometry. All angles, dihedrals and other bond distances were optimized except for bond-lengths constituting the middle guanine (assumed to be the cation radical) in 5'-GGG-3' using the ω b97xd-PCM/6-31G** level of theory. This partially optimized geometry was then fully optimized at the same level of theory. The spin density (hole) was found to localize on the middle G but the energy of this structure (Figure 4(b)) was 0.5 kcal/mol higher in energy than found for the hole at the 5'-G site shown in Figure 4(a). (ii) The second calculation we performed used the same procedure of optimization used in (i) for the cation radical on the 3'-G in 5'-GGG-3'. We found that this structure (Figure 4(c)) is 0.36 kcal/mol higher in energy than found for the hole at the 5'-G site (Figure 4(a)). The spin density plots for all three structures are presented in

Figure 4. So there appears to be a small energetic preference for the hole localization at the 5'-G site over the middle and 3'-G sites. The coordinates of the optimized structures are provided in the supporting information.

Experimental work employing ESR reported the distribution of localized holes in one-electron oxidized $d[\text{GGGCC}]_2$ and $d[\text{TGGGCCCA}]_2$ by selective deuterium substitution at the C8 position of guanine (8-deuterioguanine (G^*)).⁴⁶ In these experiments, three independent dsDNA oligomers with G^* substitutions at each G in $d[\text{GGGCC}]_2$ were investigated, specifically, (i) $d[\text{G}^*\text{GGGCC}]_2$ (ii) $d[\text{GG}^*\text{GGCC}]_2$ and (iii) $d[\text{GGG}^*\text{CCC}]_2$.⁴⁶ From the ESR experiment at 155 K, it was found that $60\% \pm 10\%$

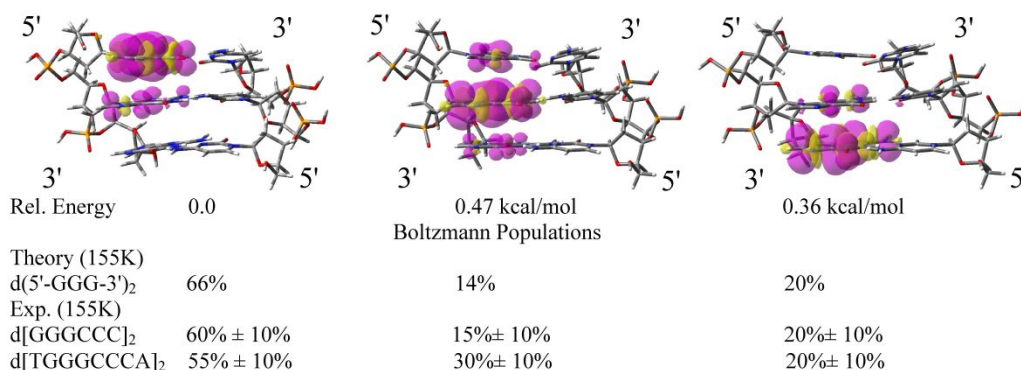


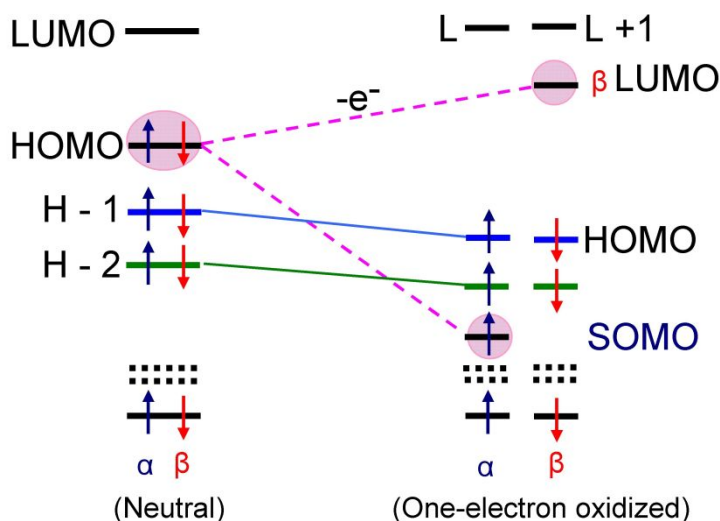
Figure 4- Spin density distribution plots of one-electron oxidized $ds(5'-\text{GGG}-3')$ calculated using the $\omega\text{b97xd-PCM}/6-31\text{G}^{**}$ method. (a) fully optimized cation radical (adiabatic) in which spin is localized on 5'-G. (b) Fully optimized cation radical (adiabatic local minimum) in which spin is mainly localized on the middle G. and (c) Fully optimized cation radical (adiabatic local minimum) in which spin is mainly localized on the 3'-G. The relative stability of structures (b) and (c) with respect to the most stable structure (a) are 0.5 and 0.4 kcal/mol, respectively. A comparison of the Boltzman population of each structure is also given along with the experimental values found for two oligomers at 155K.⁴⁶

of $(d[\text{G}^*\text{GGGCC}]_2)^{+\bullet}$ oligomers have a 5'- G^* localized hole. While $15\% \pm 10\%$ of $(d[\text{GG}^*\text{GGCC}]_2)^{+\bullet}$ oligomers have a hole localized on the middle G^* . Finally, $20\% \pm 10\%$ of $(d[\text{GGG}^*\text{CCC}]_2)^{+\bullet}$ oligomers have a 3'- G^* localized hole⁴⁶. The addition of a T before the 5'-G in $(d[\text{TGGGCCCA}]_2)^{+\bullet}$ was found to shift localization from the 5'-G to the central G, as expected⁴⁶.

Our calculations for the one-electron oxidized –GGG– stack predict three structures separated by less than 0.5 kcal/mol, see Figure 4. Thus, each one is expected to be present in experiments at 155 K⁴⁶ with small differences in energy lead to relative Boltzmann populations of each structure shown in Figure 4. The Boltzmann calculated population of structure shown in Figure 4(a) is 66%, for structure shown in Figure 4(b) is 14% and for structure shown in Figure 4(c) is 20%. These calculated populations are approximate as they are calculated using the electronic energy only, but they agree well with the ESR study⁴, perhaps, fortuitously owing to the errors inherent in both experiment and theory.

SOMO-HOMO level switching- Conventionally, it is supposed that the singly occupied molecular orbital (SOMO) should be the highest occupied molecular orbital according to the aufbau principle. However, in recent years, many studies including theory and experiment pointed out the violation of the aufbau principle for many radicals in which the SOMO is found to be energetically lower in energy than the doubly occupied HOMO.^{9,55–61,78–80} Thus, electron addition or removal to such type of radicals produces polyradicals which have interesting conductive and magnetic properties.⁶⁰ Scheme 2 shows diagrammatically how one electron oxidation can lead to SOMO to HOMO level switching. The ω b97xd-PCM/6-31G** calculated MOs of neutral and one-electron oxidized ds(5'-GGG-3') is presented in Figure S2 in the supporting information, while the ω b97xd-PCM/6-31++G** calculated MOs are presented in Figure 5. In Figure 5, we see that the HOMO of neutral ds(5'-GGG-3') is mainly delocalized on 5'-G and on the middle G and on one-electron oxidation (electron removal) the HOMO of neutral (see Figure 5) should be the SOMO which, according to aufbau principle, should be the highest occupied MO. But from the analysis of the MOs of one-electron oxidized -GGG-stack, we see that the SOMO is buried below two levels of doubly occupied MOs, see Figure 5. The burial of the SOMO below the HOMO has important consequences and it dictates that second ionization will not occur from SOMO but from HOMO which produces a diradical in the triplet^{9,61} or in open-shell singlet^{60,81} ground state. Similarly, SOMO to HOMO level inversion for one-electron oxidized ds(5'-G8OGG-3') was also found and the results are presented in Figures S3 and S6 in the supporting information.

Simultaneous two-electron oxidations within DNA were proposed earlier by Bernhard to account for products formed in nonradical processes.⁸²⁻⁸³



Scheme 2- Diagram showing the electronic configuration (α - and β -MOs) of a neutral parent molecule and its one-electron oxidized radical. In the neutral molecule, each MO is doubly occupied; however, on one-electron oxidation (removal of an electron), α - and β -MOs rearranged independently. Removal of an electron from the HOMO of the neutral molecule splits the HOMO of the neutral molecule into β -LUMO and α -SOMO, with the SOMO buried below the filled MOs. As expected, the SOMO and the β -LUMO have near identical wave functions. HOMO = highest occupied molecular orbital; LUMO = lowest unoccupied molecular orbital; and SOMO = singly occupied molecular orbital. Blue and red arrows represent α and β spin of an electron, respectively.

To test our hypothesis that SOMO to HOMO level inversion leads to a triplet state on further oxidation, we performed single point calculations for the energies of doubly oxidized $ds(5'-GGG-3')$ and $ds(5'-G8OGG-3')$ stacks in singlet and in triplet states using $\omega b97xd-PCM/6-31G^{**}$ and $\omega b97xd-PCM/6-31++G^{**}$ level of theories using the optimized structures of $ds(5'-GGG-3')^{*+}$ and $ds(5'-G8OGG-3')^{*+}$. Our calculations show that indeed the triplet states of $ds(5'-GGG-3')^{2+}$ and $ds(5'-G8OGG-3')^{2+}$ are more stable than their singlet state by 10 – 20 kcal/mol (see Figures S10 – S13 in the supporting information).

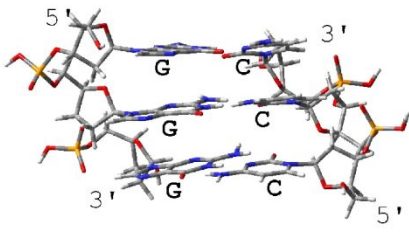
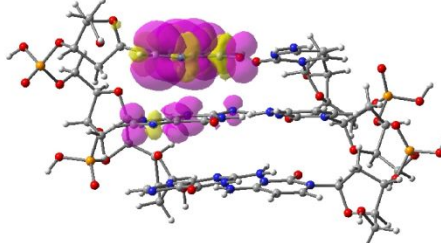
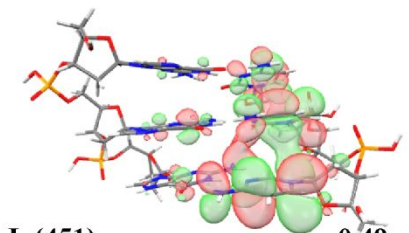
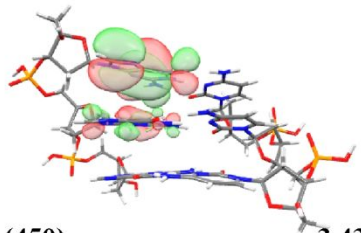
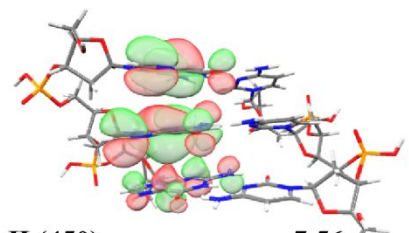
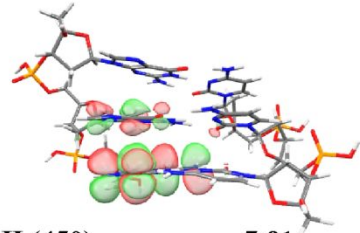
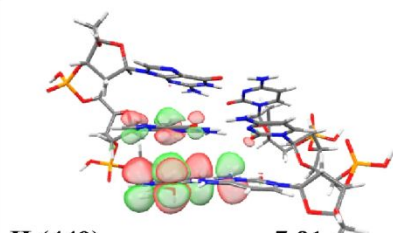
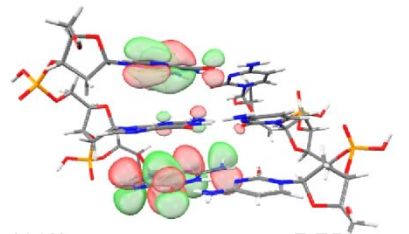
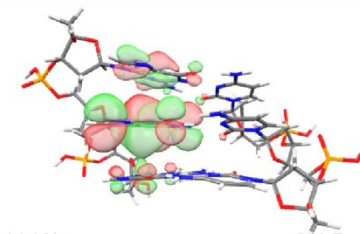
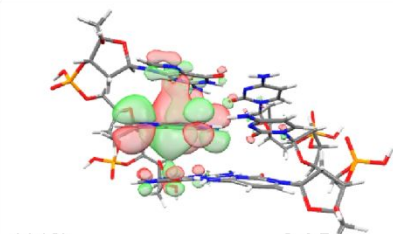
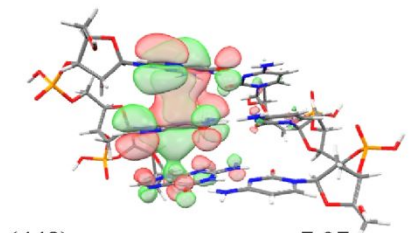
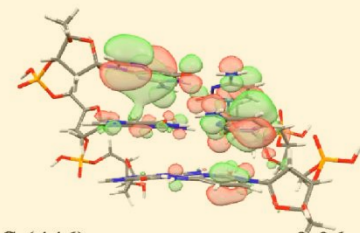
ω B97XD-PCM/6-31++G**// ω B97XD-PCM/6-31G**		
Neutral ds(5'-GGG-3')	One-electron oxidized ds(5'-GGG-3')	
	Spin 	
 L (451) 0.49		 L (450) -3.43
 H (450) -7.56	 H (450) -7.81	 H (449) -7.81
 (449) -7.75	 (449) -8.05	 (448) -8.05
 (448) -7.97	 S (446) -9.06	
MO (α, β)	α	β

Figure 5- ω b97xd-PCM/6-31++G**// ω b97xd-PCM/6-31G** calculated molecular orbital of optimized neutral ds(5'-GGG-3') and spin density and α - and β -MOs of optimized one-electron oxidized ds(5'-GGG-3') are shown. MOs energies are in eV. In the figure H, L and S designate the highest occupied molecular orbital (HOMO), the lowest unoccupied molecular orbital (LUMO) and singly occupied molecular orbital (SOMO), respectively. Note that the SOMO is below four filled single occupied MOs.

Conclusions

The present study shows that stacks of -GGG- in ds(5'-GGG-3') have a lower ionization potential than single guanine in DNA⁴³ by ca. 0.3 V. However, the presence of the damaged base, 8OG, in ds(5'-G8OGG-3') results in a low ionization potential (see Table 1) and thus act as a global sink as a hole trap as found experimentally¹⁰⁻¹⁴. The degree of solvent relaxation and its effect on spin localization/delocalization on ionization were for the first time calculated by us for ds(5'-GGG-3') and ds(5'-G8OGG-3') considering NEPCM and EQPCM approaches shown in scheme 1. Our calculations using ω b97xd-PCM/6-31G** and ω b97xd-PCM/6-31++G** level of theories show that the solvent relaxation energy (λ_1) for ionized -GGG- and -G8OGG- stacks are the same (ca. 0.7 eV, see Table 1) as the nature of spin density distributions in both the systems are similar (π -MOs delocalized on base, see Figures 1 - 3). This supports the conclusion drawn in an earlier study by Schroeder et al.⁶⁹ for one-electron oxidized nucleosides and nucleotides. The one-electron oxidation potentials (E°) of G and 8OG have been estimated using theory^{69,84} and experiment^{1-5,11,69,70} but not for -GGG- and -G8OGG-stacks in DNA. Our calculated E° of -GGG- and -G8OGG- stacks are 1.2 V and 0.9 V, respectively, which are lower than their corresponding monomer by ca. 0.3 V.

The spin density in the -GGG- cation radical stack using NEPCM in the vertical state (see Figures 1(a) and 2(a)) is delocalized on 5'-G (ca. 30%) and on the middle G (65%). But, as solvent relaxes (EQPCM) in the vertical state, the spin density in the -GGG- cation radical stack transfers from the middle G towards 5'-G, see Figures 1(b) and 2(b); and, finally in the adiabatic state, the spin -GGG- cation radical is almost completely localized at 5'-G (90%) as observed in previous studies.^{39,44-51} Localization of the hole at the 5'-G in ds(5'-GGG-3') cation radical is found to be energetically preferred to the hole localization at the middle G by only 0.5 kcal/mol and by 0.4 kcal/mol to the hole localization at the 3'-G (Figure 4). The calculated relative populations show a preference for hole localization at the 5'-G but show significant hole localization at both middle G and 3'-G as found in ESR experiments at 155 K⁴⁶.

Our calculated localized spin density at the 5'-G site in one-electron oxidized -GGG- stacks does not agree with the proposal of Capobianco et al.⁴² that the reduction in

redox potential with the number of Gs was a result of the delocalization of the hole over the guanine-rich single- and double-stranded oligonucleotides containing up to six consecutive guanines. This work and our previous theoretical work³⁷ agree that the drop in oxidation potential with number of Gs is expected but show that the hole is localized in the adiabatic state in each case. In the context of delocalized spin in the vertical states, an important question arises: *are vertical states chemically reactive?* Vertical ionized states are very short lived and usually react only after they are thermalized which occurs on the timescale of 10^{-12} - 10^{-9} s.^{85,86} It is interesting that this work confirms that the hole can localize at each of the Gs in GGG with the 5' site favored. For oxidized -G8OGG- stacks, the spin is localized mainly on 8OG in vertical as well as in the adiabatic state. Finally, we have previously found that SOMO to HOMO level inversion is a general phenomenon that occurs in many radicals^{9,58-61} including one-electron oxidized DNA systems (Scheme 2, Figure 5). In this work, we find that the SOMO is buried below several levels of doubly occupied HOMOs. This has important implications in high LET (linear energy transfer) radiation which often produces two one-electron ionizations within a short-range.^{87,88} For such species with their SOMO buried beneath their HOMO, a second ionization forms a triplet state whose chemistry is likely to be quite different than that of the doublet state resulting from a single oxidation.⁶¹

Conflicts of interest

The authors declare that there are no conflicts.

Acknowledgements

MDS, AA and AK thank the National Cancer Institute of the National Institutes of Health (Grant RO1CA045424) for support. AA and MDS thank REF, CBR at OU for support. DMC thanks the Extreme Science and Engineering Discovery Environment (XSEDE) allocation number MCB150023 for computer time. AA thanks the National Science Foundation under Grant No. CHE-1920110.

References

- 1 C. von Sonntag, Free-radical-induced DNA damage and its repair: a chemical perspective, Springer, Berlin, 2006.
- 2 A. Kumar and M. D. Sevilla, Proton-Coupled Electron Transfer in DNA on Formation of Radiation-Produced Ion Radicals, *Chem. Rev.*, 2010, **110**, 7002–7023.

- 3 S. Steenken, and S. V. Jovanovic, How Easily Oxidizable Is DNA? One-Electron Reduction Potentials of Adenosine and Guanosine Radicals in Aqueous Solution, *J. Am. Chem. Soc.*, 1997, **119**, 617–618.
- 4 N. S. Hush, and A. S. Cheung, Ionization potentials and donor properties of nucleic acid bases and related compounds, *Chem. Phys. Lett.*, 1975, **34**, 11–13.
- 5 V. M. Orlov, A. N. Smirnov and Ya. M. Varshavsky, Ionization potentials and electron-donor ability of nucleic acid bases and their analogues, *Tetrahedron Lett.*, 1976, **17**, 4377–4378.
- 6 K.-W. Choi, J.-H. Lee and S. K. Kim, Ionization Spectroscopy of a DNA Base: Vacuum-Ultraviolet Mass-Analyzed Threshold Ionization Spectroscopy of Jet-Cooled Thymine, *J. Am. Chem. Soc.*, 2005, **127**, 15674–15675.
- 7 A. Peluso, T. Caruso, A. Landi, and A. Capobianco, The Dynamics of Hole Transfer in DNA. *Molecules* **2019**, *24*, 4044.
- 8 A. Kumar, V. Pottiboyina and M. D. Sevilla, One-Electron Oxidation of Neutral Sugar Radicals of 2'-Deoxyguanosine and 2'-Deoxythymidine: A Density Functional Theory (DFT) Study, *J. Phys. Chem. B*, 2012, **116**, 9409–9416.
- 9 A. Kumar and M. D. Sevilla, Proton Transfer Induced SOMO-to-HOMO Level Switching in One-Electron Oxidized A-T and G-C Base Pairs: A Density Functional Theory Study, *J. Phys. Chem. B*, 2014, **118**, 5453–5458.
- 10 L. I. Shukla, A. Adhikary, R. Pazdro, D. Becker and M. D. Sevilla, Formation of 8-oxo-7,8-dihydroguanine-radicals in γ -irradiated DNA by multiple one-electron oxidations, *Nucleic Acids Res.*, 2004, **32**, 6565–6574.
- 11 S. Steenken, S. V. Jovanovic, M. Bietti and K. Bernhard, The trap depth (in DNA) of 8-oxo-7, 8-dihydro-2'-deoxyguanosine as derived from electron-transfer equilibria in aqueous solution, *J. Am. Chem. Soc.*, 2000, **122**, 2373–2374.
- 12 S. M. Gasper and G. B. Schuster, Intramolecular Photoinduced Electron Transfer to Anthraquinones Linked to Duplex DNA: The Effect of Gaps and Traps on Long-Range Radical Cation Migration, *J. Am. Chem. Soc.*, 1997, **119**, 12762–12771.
- 13 Z. Cai and M. D. Sevilla, Electron and Hole Transfer from DNA Base Radicals to Oxidized Products of Guanine in DNA, *Radiat. Res.*, 2003, **159**, 411–419.
- 14 R. P. Hickerson, F. Prat, J. G. Muller, C. S. Foote and C. J. Burrows, Sequence and Stacking Dependence of 8-Oxoguanine Oxidation: Comparison of One-Electron vs Singlet Oxygen Mechanisms, *J. Am. Chem. Soc.*, 1999, **121**, 9423–9428.
- 15 A. Reuther, D. N. Nikogosyan and A. Laubereau, Primary Photochemical Processes in Thymine in Concentrated Aqueous Solution Studied by Femtosecond UV Spectroscopy, *J. Phys. Chem.*, 1996, **100**, 5570–5577.
- 16 D. N. Nikogosyan, A. A. Oraevsky, V. S. Letokhov, Z. Kh. Arbieva and E. N. Dobrov, Two-step picosecond UV excitation of polynucleotides and energy transfer, *Chem. Phys.*, 1985, **97**, 31–41.

- 17 S. Marguet, D. Markovitsi and F. Talbot, One- and Two-Photon Ionization of DNA Single and Double Helices Studied by Laser Flash Photolysis at 266 nm, *J. Phys. Chem. B*, 2006, **110**, 11037–11039.
- 18 R. Arce, L. Marínez and E. Danielsen, The photochemistry of adenosine: intermediates contributing to its photodegradation mechanism in aqueous solution at 298 K and characterization of the major product, *Photochem. Photobiol.*, 1993, **58**, 318–328.
- 19 L. P. Candeias and S. Steenken, Ionization of purine nucleosides and nucleotides and their components by 193-nm laser photolysis in aqueous solution: model studies for oxidative damage of DNA, *J. Am. Chem. Soc.*, 1992, **114**, 699–704.
- 20 S. K. Kim, W. Lee and D. R. Herschbach, Cluster Beam Chemistry: Hydration of Nucleic Acid Bases; Ionization Potentials of Hydrated Adenine and Thymine, *J. Phys. Chem.*, 1996, **100**, 7933–7937.
- 21 H. Fernando, G. A. Papadantonakis, N. S. Kim and P. R. LeBreton, Conduction-band-edge ionization thresholds of DNA components in aqueous solution, *Proc. Natl. Acad. Sci.*, 1998, **95**, 5550–5555.
- 22 C. E. Crespo-Hernández, R. Arce, Y. Ishikawa, L. Gorb, J. Leszczynski and D. M. Close, Ab Initio Ionization Energy Thresholds of DNA and RNA Bases in Gas Phase and in Aqueous Solution, *J. Phys. Chem. A*, 2004, **108**, 6373–6377.
- 23 D. M. Close, Calculation of the Ionization Potentials of the DNA Bases in Aqueous Medium, *J. Phys. Chem. A*, 2004, **108**, 10376–10379.
- 24 D. M. Close, C. E. Crespo-Hernández, L. Gorb and J. Leszczynski, Ionization Energy Thresholds of Microhydrated Adenine and Its Tautomers, *J. Phys. Chem. A*, 2008, **112**, 12702–12706.
- 25 P. Slavíček, B. Winter, M. Faubel, S. E. Bradforth and P. Jungwirth, Ionization Energies of Aqueous Nucleic Acids: Photoelectron Spectroscopy of Pyrimidine Nucleosides and ab Initio Calculations, *J. Am. Chem. Soc.*, 2009, **131**, 6460–6467.
- 26 E. Pluhařová, P. Jungwirth, S. E. Bradforth and P. Slavíček, Ionization of Purine Tautomers in Nucleobases, Nucleosides, and Nucleotides: From the Gas Phase to the Aqueous Environment, *J. Phys. Chem. B*, 2011, **115**, 1294–1305.
- 27 E. Pluhařová, P. Slavíček and P. Jungwirth, Modeling Photoionization of Aqueous DNA and Its Components, *Acc. Chem. Res.*, 2015, **48**, 1209–1217.
- 28 A. Capobianco, A. Landi and A. Peluso, Modeling DNA oxidation in water, *Phys. Chem. Chem. Phys.*, 2017, **19**, 13571–13578.
- 29 A. O. Colson, B. Besler and M. D. Sevilla, Ab initio molecular orbital calculations on DNA base pair radical ions: effect of base pairing on proton-transfer energies, electron affinities, and ionization potentials, *J. Phys. Chem.*, 1992, **96**, 9787–9794.

- 30 A. O. Colson, B. Besler and M. D. Sevilla, Ab initio molecular orbital calculations on DNA radical ions. 4. Effect of hydration on electron affinities and ionization potentials of base pairs, *J. Phys. Chem.*, 1993, **97**, 13852–13859.
- 31 A. O. Colson and M. D. Sevilla, Elucidation of Primary Radiation Damage in DNA through Application of Ab Initio Molecular Orbital Theory, *Int. J. Radiat. Biol.*, 1995, **67**, 627–645.
- 32 X. Li, Z. Cai and M. D. Sevilla, Energetics of the Radical Ions of the AT and AU Base Pairs: A Density Functional Theory (DFT) Study, *J. Phys. Chem. A*, 2002, **106**, 9345–9351.
- 33 X. Li and M. D. Sevilla, DFT Treatment of Radiation Produced Radicals in DNA Model Systems, in *Advances in Quantum Chemistry*, ed. J. R. Sabin and E. Brändas, Academic Press, 2007, vol. 52, pp. 59–87.
- 34 M. Hutter and T. Clark, On the Enhanced Stability of the Guanine–Cytosine Base-Pair Radical Cation, *J. Am. Chem. Soc.*, 1996, **118**, 7574–7577.
- 35 K. B. Bravaya, E. Epifanovsky and A. I. Krylov, Four Bases Score a Run: Ab Initio Calculations Quantify a Cooperative Effect of H-Bonding and π -Stacking on the Ionization Energy of Adenine in the AATT Tetramer, *J. Phys. Chem. Lett.*, 2012, **3**, 2726–2732.
- 36 D. M. Close, One-Electron Oxidation of Individual DNA Bases and DNA Base Stacks, *J. Phys. Chem. A*, 2010, **114**, 1860–1867.
- 37 A. Kumar and M. D. Sevilla, Density Functional Theory Studies of the Extent of Hole Delocalization in One-Electron Oxidized Adenine and Guanine Base Stacks, *J. Phys. Chem. B*, 2011, **115**, 4990–5000.
- 38 M. Rooman and R. Wintjens, Sequence and conformation effects on ionization potential and charge distribution of homo-nucleobase stacks using M06-2X hybrid density functional theory calculations, *J. Biomol. Struct. Dyn.*, 2014, **32**, 532–545.
- 39 H. Sugiyama and I. Saito, Theoretical Studies of GG-Specific Photocleavage of DNA via Electron Transfer: Significant Lowering of Ionization Potential and 5'-Localization of HOMO of Stacked GG Bases in B-Form DNA, *J. Am. Chem. Soc.*, 1996, **118**, 7063–7068.
- 40 A. Golan, K. B. Bravaya, R. Kudirka, O. Kostko, S. R. Leone, A. I. Krylov and M. Ahmed, Ionization of dimethyluracil dimers leads to facile proton transfer in the absence of hydrogen bonds, *Nat. Chem.*, 2012, **4**, 323–329.
- 41 K. B. Bravaya, O. Kostko, M. Ahmed and A. I. Krylov, The effect of π -stacking, H-bonding, and electrostatic interactions on the ionization energies of nucleic acid bases: adenine–adenine, thymine–thymine and adenine–thymine dimers, *Phys. Chem. Chem. Phys.*, 2010, **12**, 2292.
- 42 A. Capobianco, T. Caruso, A. M. D'Ursi, S. Fusco, A. Masi, M. Scrima, C. Chatgililoglu and A. Peluso, Delocalized Hole Domains in Guanine-Rich DNA Oligonucleotides, *J. Phys. Chem. B*, 2015, **119**, 5462–5466.

- 43 E. Pluhařová, C. Schroeder, R. Seidel, S. E. Bradforth, B. Winter, M. Faubel, P. Slaviček and P. Jungwirth, Unexpectedly Small Effect of the DNA Environment on Vertical Ionization Energies of Aqueous Nucleobases, *J. Phys. Chem. Lett.*, 2013, **4**, 3766–3769.
- 44 I. Saito, T. Nakamura, K. Nakatani, Y. Yoshioka, K. Yamaguchi and H. Sugiyama, Mapping of the Hot Spots for DNA Damage by One-Electron Oxidation: Efficacy of GG Doublets and GGG Triplets as a Trap in Long-Range Hole Migration, *J. Am. Chem. Soc.*, 1998, **120**, 12686–12687.
- 45 D. B. Hall, R. E. Holmlin and J. K. Barton, Oxidative DNA damage through long-range electron transfer, *Nature*, 1996, **382**, 731–735.
- 46 A. Adhikary, D. Khanduri and M. D. Sevilla, Direct Observation of the Hole Protonation State and Hole Localization Site in DNA-Oligomers, *J. Am. Chem. Soc.*, 2009, **131**, 8614–8619.
- 47 L. Blancafort and A. A. Voityuk, CASSCF/CAS-PT2 Study of Hole Transfer in Stacked DNA Nucleobases, *J. Phys. Chem. A*, 2006, **110**, 6426–6432.
- 48 K. Senthilkumar, F. C. Grozema, C. F. Guerra, F. M. Bickelhaupt and L. D. A. Siebbeles, Mapping the Sites for Selective Oxidation of Guanines in DNA, *J. Am. Chem. Soc.*, 2003, **125**, 13658–13659.
- 49 A. Adhikary and M. D. Sevilla, Comment on “Theoretical Study of Polaron Formation in Poly(G)–Poly(C) Cations,” *J. Phys. Chem. B*, 2011, **115**, 8947–8948.
- 50 Y. Yoshioka, Y. Kitagawa, Y. Takano, K. Yamaguchi, T. Nakamura and I. Saito, Experimental and Theoretical Studies on the Selectivity of GGG Triplets toward One-Electron Oxidation in B-Form DNA, *J. Am. Chem. Soc.*, 1999, **121**, 8712–8719.
- 51 A. Kumar and M. D. Sevilla, Photoexcitation of Dinucleoside Radical Cations: A Time-Dependent Density Functional Study, *J. Phys. Chem. B*, 2006, **110**, 24181–24188.
- 52 C.-S. Liu and G. B. Schuster, Base Sequence Effects in Radical Cation Migration in Duplex DNA: Support for the Polaron-Like Hopping Model, *J. Am. Chem. Soc.*, 2003, **125**, 6098–6102.
- 53 J. Wu, V. E. J. Walker and R. J. Boyd, Theoretical Study of Polaron Formation in Poly(G)–Poly(C) Cations, *J. Phys. Chem. B*, 2011, **115**, 3136–3145.
- 54 P. Diamantis, I. Tavernelli and U. Rothlisberger, Vertical Ionization Energies and Electron Affinities of Native and Damaged DNA Bases, Nucleotides, and Pairs from Density Functional Theory Calculations: Model Assessment and Implications for DNA Damage Recognition and Repair, *J. Chem. Theory Comput.*, 2019, **15**, 2042–2052.
- 55 T. Kusamoto, S. Kume and H. Nishihara, Realization of SOMO–HOMO Level Conversion for a TEMPO-Dithiolate Ligand by Coordination to Platinum(II), *J. Am. Chem. Soc.*, 2008, **130**, 13844–13845.

- 56 L. V. Slipchenko, T. E. Munsch, P. G. Wenthold and A. I. Krylov, 5-Dehydro-1,3-quinodimethane: A Hydrocarbon with an Open-Shell Doublet Ground State, *Angew. Chem. Int. Ed.*, 2004, **43**, 742–745.
- 57 T. Sugawara, H. Komatsu and K. Suzuki, Interplay between magnetism and conductivity derived from spin-polarized donor radicals, *Chem. Soc. Rev.*, 2011, **40**, 3105.
- 58 G. Gryn'ova, D. L. Marshall, S. J. Blanksby and M. L. Coote, Switching radical stability by pH-induced orbital conversion, *Nat. Chem.*, 2013, **5**, 474–481.
- 59 G. Gryn'ova and M. L. Coote, Origin and Scope of Long-Range Stabilizing Interactions and Associated SOMO–HOMO Conversion in Distonic Radical Anions, *J. Am. Chem. Soc.*, 2013, **135**, 15392–15403.
- 60 G. Gryn'ova, M. L. Coote and C. Corminboeuf, Theory and practice of uncommon molecular electronic configurations: Uncommon molecular electronic configurations, *Wiley Interdiscip. Rev. Comput. Mol. Sci.*, 2015, **5**, 440–459.
- 61 A. Kumar and M. D. Sevilla, SOMO–HOMO Level Inversion in Biologically Important Radicals, *J. Phys. Chem. B*, 2018, **122**, 98–105.
- 62 Wavefunction, Inc., <https://www.wavefun.com>, (accessed September 25, 2019).
- 63 J. Tomasi, B. Mennucci and R. Cammi, Quantum Mechanical Continuum Solvation Models, *Chem. Rev.*, 2005, **105**, 2999–3094.
- 64 J.-D. Chai and M. Head-Gordon, Long-range corrected hybrid density functionals with damped atom–atom dispersion corrections, *Phys. Chem. Chem. Phys.*, 2008, **10**, 6615–6620.
- 65 J.-D. Chai and M. Head-Gordon, Systematic optimization of long-range corrected hybrid density functionals, *J. Chem. Phys.*, 2008, **128**, 084106.
- 66 A. Kumar and M. D. Sevilla, Excited States of One-Electron Oxidized Guanine-Cytosine Base Pair Radicals: A Time Dependent Density Functional Theory Study, *J. Phys. Chem. A*, 2019, **123**, 3098 – 3108.
- 67 J. Ma, A. Kumar, Y. Muroya, S. Yamashita, T. Sakurai, S. A. Denisov, M. D. Sevilla, A. Adhikary, S. Seki and M. Mostafavi, Observation of dissociative quasi-free electron attachment to nucleoside via excited anion radical in solution, *Nat. Commun.*, 2019, **10**, 102.
- 68 M. J. Frisch, G. W. Trucks, H. B. Schlegel, G. E. Scuseria, M. A. Robb, J. R. Cheeseman, G. Scalmani, V. Barone, G. A. Petersson, H. Nakatsuji, X. Li, M. Caricato, A. V. Marenich, J. Bloino, B. G. Janesko, R. Gomperts, B. Mennucci, H. P. Hratchian, J. V. Ortiz, A. F. Izmaylov, J. L. Sonnenberg, D. Williams-Young, F. Ding, F. Lipparini, F. Egidi, J. Goings, B. Peng, A. Petrone, T. Henderson, D. Ranasinghe, V. G. Zakrzewski, J. Gao, N. Rega, G. Zheng, W. Liang, M. Hada, M. Ehara, K. Toyota, R. Fukuda, J. Hasegawa, M. Ishida, T. Nakajima, Y. Honda, O. Kitao, H. Nakai, T. Vreven, K. Throssell, J. A. Montgomery, J. E. Peralta, F. Ogliaro, M. J. Bearpark, J. J. Heyd, E. N. Brothers, K. N. Kudin, V. N. Staroverov, T. A.

- Keith, R. Kobayashi, J. Normand, K. Raghavachari, A. P. Rendell, J. C. Burant, S. S. Iyengar, J. Tomasi, M. Cossi, J. M. Millam, M. Klene, C. Adamo, R. Cammi, J. W. Ochterski, R. L. Martin, K. Morokuma, O. Farkas, J. B. Foresman and D. J. Fox, *Gaussian 16, Revision A.03*; *Gaussian.com*, Gaussian, Inc., Wallingford CT, 2016.
- 69 C. A. Schroeder, E. Pluhařová, R. Seidel, W. P. Schroeder, M. Faubel, P. Slavíček, B. Winter, P. Jungwirth and S. E. Bradforth, Oxidation Half-Reaction of Aqueous Nucleosides and Nucleotides via Photoelectron Spectroscopy Augmented by ab Initio Calculations, *J. Am. Chem. Soc.*, 2015, **137**, 201–209.
- 70 C. A. Seidel, A. Schulz and M. H. Sauer, Nucleobase-specific quenching of fluorescent dyes. 1. Nucleobase one-electron redox potentials and their correlation with static and dynamic quenching efficiencies, *J. Phys. Chem.*, 1996, **100**, 5541–5553.
- 71 S. Trasatti, The absolute electrode potential: an explanatory note, *Pure Appl. Chem.*, 1986, **58**, 955 – 966.
- 72 A. V. Marenich, J. Ho, M. L. Coote, C. J. Cramer and D. G. Truhlar, Computational electrochemistry: prediction of liquid-phase reduction potentials, *Phys. Chem. Chem. Phys.*, 2014, **16**, 15068.
- 73 A. Kumar, A. Adhikary, L. Shamoun and M. D. Sevilla, Do Solvated Electrons (eaq⁻) Reduce DNA Bases? A Gaussian 4 and Density Functional Theory-Molecular Dynamics Study, *J. Phys. Chem. B*, 2016, **120**, 2115–2123.
- 74 V. Palivec, E. Pluhařová, I. Unger, B. Winter and P. Jungwirth, DNA Lesion Can Facilitate Base Ionization: Vertical Ionization Energies of Aqueous 8-Oxoguanine and its Nucleoside and Nucleotide, *J. Phys. Chem. B*, 2014, **118**, 13833–13837.
- 75 A. Kumar and M. D. Sevilla, in *Radical and Radical Ion Reactivity in Nucleic Acid Chemistry*, ed. M. M. Greenberg, John Wiley & Sons, Inc., 2009, pp. 1–40.
- 76 A. A. Voityuk, Are Radical Cation States Delocalized over GG and GGG Hole Traps in DNA?, *J. Phys. Chem. B*, 2005, **109**, 10793–10796.
- 77 R. N. Barnett, C. L. Cleveland, A. Joy, U. Landman and G. B. Schuster, Charge Migration in DNA: Ion-Gated Transport, *Science*, 2001, **294**, 567–571.
- 78 E. R. Scerri, The trouble with the aufbau principle, *Educ Chem*, 2013, **50**, 24–26.
- 79 Y. Wang, H. Zhang, M. Pink, A. Olankitwanit, S. Rajca and A. Rajca, Radical Cation and Neutral Radical of Aza-thia[7]helicene with SOMO–HOMO Energy Level Inversion, *J. Am. Chem. Soc.*, 2016, **138**, 7298–7304.
- 80 B. L. Westcott, N. E. Gruhn, L. J. Michelsen and D. L. Lichtenberger, Experimental Observation of Non-Aufbau Behavior: Photoelectron Spectra of Vanadyl-octaethylporphyrinate and Vanadyl-phthalocyanine, *J. Am. Chem. Soc.*, 2000, **122**, 8083–8084.

- 81 M. Bendikov, H. M. Duong, K. Starkey, K. N. Houk, E. A. Carter and F. Wudl, Oligocenes: Theoretical Prediction of Open-Shell Singlet Diradical Ground States, *J. Am. Chem. Soc.*, 2004, **126**, 7416–7417.
- 82 D. M. Close, W. H. Nelson and W. A. Bernhard, DNA Damage by the Direct Effect of Ionizing Radiation: Products Produced by Two Sequential One-Electron Oxidations, *J. Phys. Chem. A*, 2013, **117**, 12608–12615.
- 83 W. A. Bernhard, in *Radical and Radical Ion Reactivity in Nucleic Acid Chemistry*, ed. M. M. Greenberg, John Wiley & Sons, Inc., 2009, pp. 41–68.
- 84 B. Thapa and H. B. Schlegel, Calculations of pK_a 's and Redox Potentials of Nucleobases with Explicit Waters and Polarizable Continuum Solvation, *J. Phys. Chem. A*, 2015, **119**, 5134–5144.
- 85 A. H. Zewail, Femtochemistry: Atomic-Scale Dynamics of the Chemical Bond, *J. Phys. Chem. A*, 2000, **104**, 5660–5694.
- 86 B. C. Garrett, D. A. Dixon, D. M. Camaioni, D. M. Chipman, M. A. Johnson, C. D. Jonah, G. A. Kimmel, J. H. Miller, T. N. Rescigno, P. J. Rossky, S. S. Xantheas, S. D. Colson, A. H. Laufer, D. Ray, P. F. Barbara, D. M. Bartels, K. H. Becker, K. H. Bowen, S. E. Bradforth, I. Carmichael, J. V. Coe, L. R. Corrales, J. P. Cowin, M. Dupuis, K. B. Eisenthal, J. A. Franz, M. S. Gutowski, K. D. Jordan, B. D. Kay, J. A. LaVerne, S. V. Lymar, T. E. Madey, C. W. McCurdy, D. Meisel, S. Mukamel, A. R. Nilsson, T. M. Orlando, N. G. Petrik, S. M. Pimblott, J. R. Rustad, G. K. Schenter, S. J. Singer, A. Tokmakoff, L.-S. Wang and T. S. Zwier, Role of Water in Electron-Initiated Processes and Radical Chemistry: Issues and Scientific Advances, *Chem. Rev.*, 2005, **105**, 355–390.
- 87 Pimblott, S. M.; Mozumder, A. Structure of Electron Tracks in Water. 2. Distribution of Primary Ionizations and Excitations in Water Radiolysis. *J. Phys. Chem.* 1991, **95**, 7291–7300.
- 88 LaVerne, J. A.; Pimblott, S. M. Electron Energy-Loss Distributions in Solid, Dry DNA. *Radiat. Res.* 1995, **141**, 208–215.

TOC

Localized hole distributions in ds(5'-GGG-3') and ds(5'-G(8OG)G-3') stacks

